Journal of Vizualized Experiemnts

TITLE:
Ex Vivo Optogenetic Interrogation of Long-Range Synaptic Transmission and Plasticity from Medial Prefrontal Cortex to Lateral Entorhinal Cortex

AUTHORS AND AFFILIATIONS:
Lisa Kinnavane[1], Paul J. Banks[1]

[1]School of Physiology, Pharmacology and Neuroscience, University of Bristol, Bristol, United Kingdom.

Email addresses of co-authors:
Lisa Kinnavane (lisa.kinnavane@bristol.ac.uk)
Paul J. Banks (paul.banks@bristol.ac.uk)

Corresponding author:
Lisa Kinnavane (lisa.kinnavane@bristol.ac.uk)

KEYWORDS:
electrophysiology, optogenetics, synaptic transmission, synaptic plasticity, rats, mice, neurons

SUMMARY:
Here we present a protocol describing viral transduction of discrete brain regions with optogenetic constructs to permit synapse-specific electrophysiological characterization in acute rodent brain slices.

ABSTRACT:
Studying the physiological properties of specific synapses in the brain, and how they undergo plastic changes, is a key challenge in modern neuroscience. Traditional *in vitro* electrophysiological techniques use electrical stimulation to evoke synaptic transmission. A major drawback of this method is its nonspecific nature; all axons in the region of the stimulating electrode will be activated, making it difficult to attribute an effect to a particular afferent connection. This issue can be overcome by replacing electrical stimulation with optogenetic-based stimulation. We describe a method for combining optogenetics with *in vitro* patch-clamp recordings. This is a powerful tool for the study of both basal synaptic transmission and synaptic plasticity of precise anatomically defined synaptic connections and is applicable to almost any pathway in the brain. Here, we describe the preparation and handling of a viral vector encoding channelrhodopsin protein for surgical injection into a pre-synaptic region of interest (medial prefrontal cortex) in the rodent brain and making of acute slices of downstream target regions (lateral entorhinal cortex). A detailed procedure for combining patch-clamp recordings with synaptic activation by light stimulation to study short- and long-term synaptic plasticity is also presented. We discuss examples of experiments that achieve pathway- and cell-specificity by combining optogenetics and Cre-dependent cell labeling. Finally, histological confirmation of the pre-synaptic region of interest is described

along with biocytin labeling of the post-synaptic cell, to allow further identification of the precise location and cell type.

INTRODUCTION:

Understanding the physiology of synapses and how they undergo plastic changes is fundamental for understanding how brain networks function in the healthy brain[1], and how they malfunction in brain disorders. The use of acute *ex vivo* brain slices allows for the recording of the electrical activity of synapses from single neurons with a high signal-to-noise ratio using whole-cell patch-clamp recordings. Control of membrane potential and straightforward pharmacological manipulation allows isolation of receptor subtypes. These recordings can be made with exquisite specificity to identify the post-synaptic neuron, including laminar and sub-regional position[2], cellular morphology[3], presence of molecular markers[4], its afferent projections[5], or even if it was recently active[6].

Achieving specificity of pre-synaptic inputs is, however, somewhat more challenging. The conventional method has used stimulation electrodes to excite the axons which run in a particular lamina. An example of this is in the hippocampus where local stimulation in the stratum radiatum activates synapses that project from the CA3 to the CA1 subfields[7]. In this instance, presynaptic specificity is achieved as CA3 input represents the sole excitatory input located within stratum radiatum which projects to CA1 pyramidal cells[8]. This high degree of input specificity achievable with conventional electrical presynaptic activation of CA3–CA1 axons is, however, an exception which is reflected in the intense study that this synapse has been subject to. In other brain regions, axons from multiple afferent pathways co-exist in the same lamina, for example, in layer 1 of neocortex[9], thus rendering input-specific presynaptic stimulation impossible with conventional stimulating electrodes. This is problematic as different synaptic inputs may have divergent physiological properties; therefore, their co-stimulation may lead to mischaracterization of synaptic physiology.

The advent of optogenetics, the genetic encoding of photosensitive membrane proteins (opsins) such as channelrhodopsin-2 (ChR2), has allowed a vast expansion of possibilities for studying isolated synaptic projections between brain regions[10,11]. Here we describe a generalizable and low-cost solution to studying long-range synaptic physiology and plasticity. The optogenetic constructs are delivered in a highly specific manner using viral vectors allowing for extremely precise control of the pre-synaptic region of interest. Efferent projections will express the light-activated channel allowing for activation of these fibers in a target region. Thus, long-range, anatomically diffused pathways that cannot be independently activated by traditional, non-specific, electrical stimulation can be studied.

We describe, as an example pathway, transduction of medial prefrontal cortex (mPFC) with adeno-associated viruses (AAVs) encoding excitatory cation-channel opsins. We then describe the preparation of acute slices from lateral entorhinal cortex (LEC), patch-clamp recordings from layer 5 LEC pyramidal neurons, and light-evoked activation of glutamatergic mPFC-LEC projections (**Figure 1**). We also describe the histological assessment of the injection site to confirm the location of the pre-synaptic region of interest and identification of post-synaptic cell morphology.

PROTOCOL:

All animal procedures were conducted in accordance with the United Kingdom Animals Scientific Procedures Act (1986) and associated guidelines as well as local institutional guidelines.

1. Stereotaxic viral injection

NOTE: The current protocol requires anatomical, but not post-synaptic cell type, specificity.

1.1. Choose the appropriate animal. Male wild-type Lister hooded rats were used in this protocol (300–350 g, approximately 3 months old).

1.2. Choose the appropriate viral construct. There are several factors to consider (see **Discussion**). The current protocol uses a virus to express the optogenetic channel $ChETA_{TC}$[12], to transduce excitatory neurons (AAV9 – CaMKIIa - ChR2(E123T/T159C) – mCherry; titer: 3.3 x 10^{13} viral genomes/mL).

1.3. Establish the coordinates and volume of injection.

1.4. Stereotaxic injection of the viral preparation

NOTE: All relevant national and institutional guidelines for the use and care of animals should be followed. The viral vectors are stereotaxically injected as previously described[13] with the following modifications.

1.4.1. Keep the viral preparation on ice during anesthetization and preparation of the animal.

1.4.2. Induce anesthesia in an anesthetic induction chamber with 4% isoflurane. Monitor the level of anesthesia indicated by slower regular breathing rate (1 Hz) and absence of pedal and corneal reflexes (test by pinching toes and lightly touching the corner of the eye, respectively; no response should be detected).

1.4.3. When the animal is fully anesthetized, use clippers to remove fur from the scalp. Switch the isoflurane flow to the nose cone of the stereotaxic frame and mount the rat in the frame. Apply lubricating eye gel to the eyes to prevent dryness during the procedure.

1.4.4. The surgery should be undertaken in aseptic conditions. Use sterile gloves and instruments throughout the procedure. Apply lidocaine ointment (5% w/w) before disinfecting the scalp with 4% w/v chlorhexidine solution, and then cover the body with a sterile drape. Using a scalpel, make a longitudinal incision approximately 15 mm in length on the scalp to expose bregma.

1.4.5. Load a Hamilton syringe into a microinjection syringe pump attached to a moveable arm mounted to the stereotaxic frame.

1.4.6. Place a 5 µL aliquot of the virus in a 0.2 mL tube and spin for a few seconds until all the volume is in the bottom of the tube. Pipette 2 µL of the viral preparation into the lid of the tube.

1.4.7. Fill the syringe with the viral preparation by first viewing the needle tip with a surgical microscope, and then manually place the bolus of the virus at the tip of the needle and withdraw the syringe plunger using the pump controls.

1.4.8. Set the pump injection volume to 300 nL and flow rate to 100 nL/min. Run the pump and confirm proper flow by observing the droplet of the virus at the needle tip. Absorb the virus on a cotton bud and gently clean the needle with 70% ethanol.

1.4.10. Using the adjuster screws on the stereotaxic frame navigate needle tip to bregma (the point on the skull where the coronal and sagittal sutures meet) and take note of the stereotaxic measurements observed on the three vernier scales on the frame. The coordinates relative to bregma of rat mPFC are anterior-posterior + 3.1 mm, mediolateral ± 0.7 mm, dorsoventral - 4.5 mm; add/subtract (as indicated) these distances from bregma coordinates, and then navigate the needle to the anterior-posterior and mediolateral coordinates and gently lower the needle onto the skull surface.

NOTE: The mPFC coordinates given above are appropriate for male lister hooded rats of 300–350 g; changes in rat strain, size may require alterations to these coordinates (see **Discussion**).

1.4.11. Raise the needle off the skull surface and mark this point with a fine-tip permanent marker pen. Make a burr hole at this point using a micro drill mounted to the stereotaxic arm.

1.4.12. Insert the needle into the brain at the pre-determined dorsoventral coordinate and infuse a pre-determined volume (for mPFC: 300 nL). Leave the needle *in situ* for 10 min to allow for the diffusion of the bolus. Upon removal of the needle, run the pump to ensure that the needle is not blocked.

NOTE: Insert and remove the needle slowly (~3 mm/min) to minimize the damage to the brain tissue and backflow of the virus into the needle tract.

1.4.13. Administer 2.5 mL of warmed sodium chloride (0.9% w/v) and glucose (5% w/v) solution subcutaneously to maintain hydration.

1.4.14. Repeat step 1.4.12. for the second hemisphere.

1.4.15. Suture the scalp incision and on completion of the procedure, administer 2.5 mL of sodium chloride and glucose solution and an appropriate, institutionally recommended, analgesic for pain management, e.g., buprenorphine or meloxicam. Do not leave the animal unattended while unconscious. Place the rat in a heated recovery box until it fully regains consciousness. Only return to the home cage with other animals once fully recovered.

1.4.16. Follow the institutional guidelines for post-operative care and housing procedures for viral-transfected rodents. Wait for at least 2 weeks for the opsin transgene to express adequately before starting the experiment.

NOTE: The time required for transduction is dependent on the distance and strength of the connection between the pre-and post-synaptic regions. For mPFC to LEC, 4–6 weeks is required.

2. Preparation of acute brain slices

NOTE: Here we describe a simple method for the preparation of brain slices which in our hands is sufficient to achieve high-quality cortical, hippocampal, and thalamic slices from adult mice and rats.

2.1. Prepare the solutions for dissection.

2.1.1. Fill a 250 mL beaker with ~200 mL of ice-cold sucrose cutting solution (189 mM sucrose, 26 mM $NaHCO_3$, 10 mM D-glucose, 5 mM $MgSO_4$, 3 mM KCl, 1.25 mM NaH_2PO_4, and 0.2 mM $CaCl_2$ made in ultrapure water (UPW) with resistivity of 18.2 MΩ cm at 25 °C) or a sufficient volume to fill the vibratome tissue chamber. Bubble with carbogen (95% O_2, 5% CO_2) and keep on ice.

2.1.2. Fill a slice collection chamber with artificial cerebrospinal fluid (aCSF; 124 mM NaCl, 26 mM $NaHCO_3$, 10 mM D-glucose, 3 mM KCl, 2 mM $CaCl_2$, 1.25 mM NaH_2PO_4, and 1 mM $MgSO_4$ made in UPW) at room temperature, bubbled with carbogen. The slice collection chamber[14] is custom made from a microcentrifuge tube rack glued onto a sheet of nylon mesh and placed into a beaker in which it is submerged in aCSF (**Figure 2A**).

2.1.3. Fill a 50 mL tube with 4% paraformaldehyde (PFA) in phosphate buffer (PB; 75.4 mM $Na_2HPO_4.7H_2O$ and 24.6 mM $NaH_2PO_4.H_2O$).

CAUTION: PFA is toxic. Use in fume hood.

2.2. Dissection of the brain.

2.2.1. Anesthetize the rat in an induction chamber using 5% isoflurane until breathing is slow and regular (~1 Hz). To ensure a sufficient level of anesthesia test for the absence of pedal and corneal reflexes.

2.2.2. Decapitate the animal using a guillotine.

2.2.3. Rapidly dissect out the entire brain as previously described[15] and transfer into sucrose cutting solution. Complete the step within 90 s of decapitation for good slice quality and successful whole-cell recording.

2.2.4. Using a metal teaspoon, pick up the brain, discard excess cutting solution, and place it onto a piece of filter paper on the benchtop.

2.2.5. Using a scalpel or razor blade, quickly remove the cerebellum and cut the cerebrum in the coronal plane approximately halfway along its length; the posterior half is the LEC tissue block. Be sure to include some excess tissue in addition to the region to be sliced for the next steps. Return both this tissue block and the remainder of the brain to the sucrose cutting solution.

2.2.6. Place a drop of cyanoacrylate glue onto a vibratome tissue stage. Spread it into a thin layer with an area slightly larger than the tissue block created in the previous step.

2.2.7. Pick up the LEC tissue block using a teaspoon, discard excess solution, and transfer onto the glue patch such that the anterior coronal cut has adhered.

2.2.8. Install the stage into the vibratome tissue chamber and quickly pour a sufficient amount of sucrose cutting solution to submerge the tissue; bubble this solution with carbogen. Orient the LEC tissue block with the ventral surface toward the blade. While ambient room lighting is insufficient to activate the opsin, avoid using additional light sources which might be present on the vibratome.

2.2.9. Cut slices of 350 µm thickness from ventral to dorsal using a high blade oscillation speed (100 Hz) and a slow blade advancement speed (0.06 mm/s). Typically, seven LEC slices can be obtained per hemisphere.

2.2.10. Transfer the slices to the slice collection chamber. Upon completion of slice collection, transfer the collection chamber to a 34 °C water bath for 1 h before returning to room temperature. Bubble with carbogen continuously. Slices will be sufficiently healthy for recording for at least 6 h.

2.2.11. Place the remainder of the brain in PFA for 48 h for post-hoc examination of injection site (see section 4).

3. Electrophysiology and optogenetic stimulation

3.1. Identification of target cell.

3.1.1. Place the slice into a submerged recording chamber at 34 °C perfused with aCSF at a rate of 2 mL/min by a peristaltic pump. Immobilize the slice using a slice anchor.

3.1.2 Under the low magnification (4x) objective of a widefield microscope using oblique infrared illumination, navigate to LEC layer 5. Measure the distance from the pial surface to the required layer.

NOTE: Oblique infrared illumination was achieved by positioning a near infra-red LED approximately 3 mm below the recording chamber coverslip at an angle of ~55° to the plane of the coverslip (**Figure 2B**). Differential interference contrast is an alternative and commonly used imaging technique for slice electrophysiology.

3.1.3. Change to a high magnification water immersion objective (40x) and identify pyramidal neurons. Mark the position of the cell on the computer monitor with tape.

NOTE: The pyramidal neurons have a roughly triangular morphology with prominent apical dendrites projecting toward the pial surface of the slice (**Figure 3A**). Cell health can be assessed by the absence of a condensed, visible nucleus and inspection of the plasma membrane which should appear smooth. It is unlikely that clear fluorescent labeling of axons by the opsin-fluorophore fusion protein will be visible when using a wide-field fluorescence microscope. To visualize axonal projections, perform immunohistochemistry post-hoc using a primary antibody against the opsin's fluorophore and amplify with a secondary antibody conjugated to a fluorophore of the same or similar wavelength.

3.2. Formation of whole-cell patch-clamp.

3.2.1. Fabricate a borosilicate glass micropipette using a pipette puller and fill with filtered intracellular recording solution (120 mM k-gluconate, 40 mM HEPES, 10 mM KCl, 2 mM NaCl, 2 mM MgATP, 1 mM MgCl, 0.3 mM NaGTP, 0.2 mM EGTA, and 0.25% biocytin made in UPW, pH 7.25, 285–300 mOsm). Place the filled micropipette in the electrode holder on the patch-clamp amplifier headstage ensuring the electrode wire is in contact with the intracellular solution.

3.2.2 Apply positive pressure by mouth by blowing hard into a mouthpiece (such as a 1 mL syringe with the plunger removed) connected by tubing to the electrode holder side port and maintain pressure by closing an in-line three-way valve. Raise the microscope objective such that a meniscus forms and insert the electrode into the meniscus until it can be seen on the microscope.

3.2.3 Open the **Seal Test** window in WinLTP[16] (or other acquisition software/oscilloscope) and with the amplifier in the voltage-clamp mode, apply a 5 mV square pulse to determine whether the pipette resistance is 3–5 MΩ.

3.2.4. Approach and touch onto the identified cell with the pipette tip; this should result in an indentation in the cell membrane (**Figure 3A; right panel**) and a small increase in pipette resistance (0.1 MΩ).

3.2.5. Release positive pressure and apply negative pressure by applying moderate suction at the mouthpiece; this should result in a vast increase in pipette resistance (>1000 MΩ). Pressure can now be left neutral. Apply negative pressure in a gradually increasing ramp until cell membrane ruptures result in whole-cell capacitance transients.

3.3. Record optogenetically evoked synaptic events.

3.3.1. Enter current-clamp configuration.

NOTE: In most instances long-range synaptic transmission is glutamatergic, therefore recording at membrane potentials close to the chloride reversal potential will best isolate AMPA receptor (AMPAR)-mediated transmission and minimize measurement of any feed-

forward inhibition (FFI) evoked. Chloride reversal is dependent on the composition of intracellular recording solution and aCSF and can be calculated using the Goldman-Hodgkin-Katz equation; for the above solutions, this was -61.3 mV. Layer 5 LEC pyramidal neurons had an average resting membrane potential of -62 mV and, where necessary, were maintained at this potential by injection of constant current. Alternatively, cells can be voltage clamped to the desired potential. To record long-range inhibitory projections[16] or to record FFI, voltage-clamp at cation reversal potential to isolate GABAergic chloride conductance. When voltage-clamping neurons at membrane potentials above action potential threshold, a cesium-based intracellular solution containing voltage-gated sodium channel blockers is used to improve voltage-clamp and prevent initiation of action potentials (130 mM $CsMeSO_4$, 10 mM HEPES, 8 mM NaCl, 5 mM QX 314 chloride, 4 mM MgATP, 0.5 mM EGTA, 0.3 mM NaGTP, 0.25% biocytin made in UPW, pH 7.25, 285–300 mOsm).

3.3.2. Using data acquisition software, send transistor-transistor logic (TTL) signals to an LED driver to activate a mounted 470 nm LED. The mounted LED is directed into the microscope light path using filter cubes and appropriate optics (**Figure 2B**) to apply light pulses to the slice *via* the 40x objective to evoke optogenetic excitatory post-synaptic potentials (oEPSPs).

NOTE: Light pulses can be applied perisomatically/over the dendrites, which will result in activation of opsins in the axons and presynaptic bouton, or the investigator can move the objective to axons away from the recorded cell to avoid over-bouton stimulation (see **Discussion**). Maximal oEPSP amplitude depends on the strength of the synaptic projection, the efficacy of viral injections, and opsin used. oEPSPs can be titrated to the desired amplitude by varying light intensity and/or duration[18]; varying the duration of light pulses (typical duration between 0.2–5 ms at maximal LED power output, which results in 4.4 mW/mm light density[19]) gives more consistent oEPSP amplitudes than altering the power output of the LED.

3.3.3. Investigate presynaptic release properties (change in voltage) by delivering trains of multiple light pulses with differing inter-stimulus intervals (**Figure 3E**); care should be taken while interpreting optogenetically evoked transmission (see **Discussion**).

3.3.4. Investigate long-term plasticity either by repetitively evoking oEPSPs[19] or application of ligands. Monitor oEPSP amplitude for 5–10 min to ensure stability before induction of plasticity, and then monitor until a stable amplitude is reached (typically 30–40 min).

NOTE: Current opsins are not capable of reliably evoking multiple action potentials at high frequencies, e.g., 100 stimuli delivered at 100 Hz, as is typically used to induce LTP.

3.3.5. To confirm oEPSPs are monosynaptic, perform over-bouton activation of the transduced pathway by positioning the objective over the dendritic arbor and stimulating in the presence of 0.5 µM tetrodotoxin and 100 µM aminopyridine. Application of tetrodotoxin will abolish transmission if the responses are action potential-dependent and subsequent inclusion of aminopyridine will partially restore transmission if the oEPSPs are generated monosynaptically[19,20].

3.3.6. To allow biocytin to fill the neuron, wait for at least 15 min after entering the whole-cell configuration. In voltage-clamp, monitor membrane capacitance and input resistance.

3.3.7. Slowly withdraw the pipette along the approach angle away from the soma of the cell, observing the slow disappearance of capacitance transients and membrane current indicating the re-sealing of the cell membrane and formation of an outside-out patch at the pipette tip. Note the orientation of the slice and the location of the cell(s) within the slice. Put the slice into PFA in a 24-well plate and incubate overnight at 4 °C, and then transfer to 0.1 M PB.

NOTE: Slices can be stored for up to a week. If longer storage is required, change the PB regularly or use sodium azide containing PB (0.02%–0.2% of sodium azide).

4. Histology

4.1. Slicing injection site

4.1.1. Following fixation, cryoprotect the tissue in 30% sucrose (w/v) in PB until it sinks (it will initially float in the sucrose solution), usually overnight at room temperature or 24–48 h at 4 °C.

4.1.2. Using optimal cutting temperature (OCT) medium, attach a block of tissue to cryostat the specimen disk. Freeze the tissue block following steps 4.1.3 to 4.1.4.

4.1.3. Place isopentane in an appropriate container. Submerge just the specimen disk, ensuring the tissue is above the level of the isopentane. Lower the container of isopentane into liquid nitrogen (or dry ice) and allow the tissue to freeze.

4.1.4. Once completely frozen (the entire tissue block becomes pale and hard), leave the tissue block in the cryostat chamber at -20 °C for 30 min to allow the temperature of the block to equilibrate.

4.1.5. Cut 40 µm thick sections in the cryostat at -20 °C. Use a fine paintbrush to guide the sections off the blade. Adhere frozen sections to a room temperature, poly-L-lysine coated, glass microscope slide by touching the slide to the sections.

4.1.6. Add around 150 µL of mounting medium to each slide and cover with a coverslip; remove any air bubbles by gently pressing on the coverslip. Cover the slides to protect against photobleaching and air-dry at room temperature for at least 12 h (or overnight). Using a fluorescence microscope, examine the location of the viral injection site.

4.2. Biocytin staining protocol

NOTE: This protocol can be applied to thick sections; slices do not need to be re-sectioned.

4.2.1. Wash the brain slices with phosphate-buffered saline (PBS; 137 mM NaCl, 2.7 mM KCl, 10 mM Na_2HPO_4, and 1.8 mM KH_2PO_4) six times for 10 min per wash. Use a transfer pipette to empty the wells after each step.

4.2.2. Incubate the slices in 3% H_2O_2 (w/v) in PBS for 30 min to block any endogenous peroxidase activity. This generates oxygen bubbles.

4.2.3. Wash the brain slices with PBS six times for 10 min per wash or until no further oxygen bubbles are visible. Incubate the brain slices in 1% (v/v) avidin-biotinylated HRP complex (ABC) solution in PBS containing 0.1% (v/v) Triton X-100 at room temperature for 3 h.

4.2.4. Wash the brain slices with PBS six times for 10 min per wash.

4.2.5. Incubate each slice in 3,3'-Diaminobenzidine (DAB) solution for several minutes until the biocytin staining of neuronal structures becomes visible (takes around 5–10 min).

CAUTION: DAB is toxic. Use in fume hood.

NOTE: DAB incubation times can be unpredictable, monitor the tissue closely as the color develops.

4.2.6. Stop the reaction by transferring the slices in cold (4 °C) PBS. Wash the brain slices with PBS six times for 10 min per wash. Use a brush to mount the brain slices onto the adhesive, poly-L-lysine coated glass microscope slides.

4.2.7. Remove all excess PBS with a clean tissue. Cover each slice with about 200 µL of mounting medium; cover with coverslips and gently press on the coverslip to push out air bubbles. Air-dry at room temperature for at least 12 h (or overnight). Using a light microscope, examine the location and morphological details of the cell(s).

NOTE: Biocytin can alternatively be visualized using fluorophore-conjugated streptavidin; however, imaging may require resectioning or the use of a confocal microscope[21].

REPRESENTATIVE RESULTS:

In this protocol, we describe how to study long-range synaptic physiology and plasticity using viral delivery of optogenetic constructs. The protocol can be very easily adapted to studying almost any long-range connection in the brain. As an example, we describe the injection of AAVs encoding an opsin into rat mPFC, the preparation of acute slices from LEC, patch-clamp recordings from layer 5 LEC pyramidal neurons, and light-evoked activation of mPFC terminals in LEC (**Figure 1**).

A healthy pyramidal cell was located and patched (e.g., **Figure 3A**). In the present mPFC to LEC example, the post-synaptic cells were not labeled; if post-synaptic cell identification is required, a cell expressing the fluorescent marker should be localized using widefield optics (e.g., **Figure 3B**). The health of the cell should be assessed by infrared optics before experimentation. To activate mPFC axons in LEC, an LED was placed directly over layer 5 cell soma and proximal dendrites *via* the microscope objective (**Figure 1**), single light pulses of 2 ms resulted in simple waveform oEPSPs (**Figure 3C**); the peak amplitude of the oEPSP can be measured. To examine short-term plasticity of the synapse, 5, 10, and 20 Hz trains of light stimulation were applied (**Figure 3E**). To investigate long-term plasticity, after monitoring

baseline oEPSP amplitude for 10 min the cholinergic agonist, carbachol, was added to the circulating aCSF for 10 min. This caused long-term depression that was still evident 40 min after removal of the ligand (**Figure 3D**).

Following electrophysiological recording experiments, the brain tissue containing the viral injection site was sectioned and the length of the injection site was examined (**Figure 4A**). The fluorescent reporter, mCherry, is localized to the deeper layers of the prelimbic and infralimbic cortex (constituent regions of rodent mPFC). These layers were targeted as the projection to LEC has been shown to originate predominantly from the deeper cortical layers[22]. mCherry positive fibers can also be seen joining the white matter tract. In a pilot experiment to optimize viral injection placement, 40 µm sections of LEC were taken and examined; mCherry positive fibers can be seen in layer 5 of LEC (**Figure 4B**). Finally, the biocytin filled cell was stained, allowing its location and morphology to be confirmed (**Figure 4C,D**).

DISCUSSION:

The protocol presented here describes a method to explore highly specific long-range synaptic projections using a combination of stereotaxic surgery to deliver AAVs encoding optogenetic constructs, and electrophysiology in acute brain slices (**Figure 1**). Together these techniques offer tools to characterize the physiology and plasticity of brain circuitry with high precision in long-range and anatomically diffuse pathways that were previously inaccessible using traditional, non-specific, electrical stimulation. Combination with cell-specific molecular markers allows characterization of projections from one brain region to different defined cell populations in another region[23].

To take full advantage of the highly precise nature of this technique, it is essential to verify pathway specificity. This is done in several steps; during recording, ensure the synapse under investigation is mono-synaptic (step 3.3.5). Following this, histologically examine the injection site to ensure the virus is confined to the intended pre-synaptic region of interest and assess the location and morphology of the biocytin stained post-synaptic cell to ensure it is as anticipated.

Virus selection and achieving cellular specificity

The technique is highly adaptable and suitable for use in both mice and rats. Experiments requiring anatomical specificity can be performed with wild-type rodents. Experiments requiring post-synaptic cell type specificity may require a genetically modified rodent strain if cells are not identifiable based on morphology or location. For example, to target parvalbumin (PV) expressing interneurons, a PV-Cre knock-in transgenic mouse line in which Cre-recombinase is expressed in PV-expressing neurons could be used. To visualize these cells, the PV-Cre line can be crossed with a reporter mouse line to express a fluorescent protein following Cre-mediated recombination. Alternatively, a Cre-dependent fluorescent reporter gene can be introduced virally. ChR2-fluorophore fusion proteins are restricted to the cell membrane and may appear as an outline of the neuron when viewed with widefield microscopy in acute slices making identification of cells for whole-cell recording more challenging than using cytosolic fluorophores. If ChR2 is being used to identify cells, separation of ChR2 and fluorophore can be achieved using bicistronic vectors[24]. If using a fluorescent reporter to identify target neurons for whole-cell recording, its excitation

wavelength should ideally not overlap with the activation wavelength of the opsin; this will avoid prolonged activation of transduced afferents while searching for neurons to record from. Likewise, pre-and post-synaptic reporters should be spectrally separate. Common reporters are mCherry, green fluorescent protein (GFP), and enhanced yellow fluorescent protein (eYFP).

The viral construct used has several different components, each can impact the success of the experiment and so consideration must be given to each element. Primary importance should be given to the choice of opsin. For presynaptic activation, the ideal opsin has large photocurrents (to reliably bring axons to action potential threshold), rapid on- and off-kinetics, and a slow rate of desensitization to allow high-frequency repeated stimulation. As a rule, rapid kinetics often come at the cost of smaller photocurrents[25]; however, molecular screening and engineering have provided opsins with large photocurrents. The current protocol uses ChR2(E123T/T159C) $ChETA_{TC}$[12], however Chronos[26], CheRiff[27], $oChIEF_{AC}$[28], and ChRmine[29] are also suitable. Additionally, excitatory opsins with either red-shifted (ChrimsonR)[26] or violet-shifted (CheRiff) activation wavelengths exist, which may be required to avoid overlap with excitation spectra of fluorophores used for cell identification (see below).

The serotype of AAVs can affect the vector's ability to transduce different brain regions and cell types as well as the extent of axonal transport in both the anterograde and retrograde directions[30]. Serotypes commonly used for neuronal transduction are 1, 2, 5, 8, and 9. A literature search may give an indication of which serotype has been used successfully in any given region. For example, AAV9 has been recommended for the transduction of cortical neurons[31].

The promotor allows for the specification of the cell type in which the opsin will be expressed. Promotors fall into several classes. General promotors, e.g., CAG or EF1a, result in expression in most cell types. Neuron-specific promotors, e.g., synapsin, generate expression in all neuron types. CaMKIIa is commonly used to restrict expression to excitatory neurons although it has been shown to be leaky—some expression has been observed in interneurons[32]. The mDlx enhancer element limits expression to GABAergic interneurons[33]. Pre-synaptic cell type specificity can be achieved using a Cre-mouse line (as described above for the post-synaptic cell). In this case, a Cre-dependent genetic construct will be required to limit opsin expression to Cre-expressing cells.

Titre is the number of viral particles in the viral preparation. Again, a literature search may give an indication of a titre that has generated sufficient transduction in a particular region. When using a Cre-dependent system, the titre may be particularly important as high viral titres can transduce expression in non-Cre-expressing cells[34].

Optimization of virus delivery

Precise viral delivery to the region of interest is of critical importance to this approach. Injection coordinates of the pre-synaptic region can be estimated by consulting the literature and/or a brain atlas for the appropriate species[35,36]. The experimenter should then take time to optimize and refine the precise injection coordinates and volume used to ensure that the viral injection is restricted to their presynaptic region of interest. This is especially critical

when neighboring regions also project to the recording site. We recommend using small volumes of the virus as an effective method of doing this. If a particularly small injection site is required, the use of glass micropipettes in place of a syringe and needle may be advantageous[13]. Leaving the injection needle *in situ* for an adequate period and slow withdrawal of the injection needle is critical to prevent the virus from escaping into the needle tract. To confirm the accuracy of injections, it is best practice to histologically verify the injection site of each animal used through electrophysiology where possible and exclude data where viral transduction is off-target. In our hands, the protocol described above has proven to be generalizable to many different long-range connections, including projections from ventral midline thalamic nuclei, hippocampus, mediodorsal thalamus, and LEC to PFC; projections from PFC to LEC and mediodorsal thalamus; projections from LEC and ventral midline thalamic nuclei to hippocampus (Zafar Bashir lab, University of Bristol, unpublished observations[19]). Optogenetic labeling of these different pathways has merely required refinement of injection coordinates and volumes.

Protocol limitations

Rapid dissection of the brain and careful slicing are critically important for the success of these experiments. The slicing protocol described here yields healthy acute slices without adaptation for different brain regions; however, variation in slicing medium and post-slicing incubation temperature described elsewhere[28] have been reported to improve slice health further. Moreover, we have also been able to take acute slices from two brain regions following viral transduction of a single area, thus reducing the number of animals used. We have found that in anatomically dense pathways, periods as short as 7 days between viral transduction and recording are sufficient to evoke robust oEPSPs of suitable magnitude for whole-cell patch-clamp recordings. In longer-range or more sparse projections, longer delays are advantageous.

Care should be exercised when interpreting the results of optogenetically evoked activity, particularly with respect to short-term plasticity. Previous results have shown that optogenetically evoked transmission may undergo more pronounced synaptic depression upon repeated stimulation than electrical stimulation, which may arise due to a number of factors. Firstly, opsin desensitisation[25] may lead to a reduced number of presynaptic neuron spiking leading to reduced postsynaptic responses. The improved channel kinetics of recently discovered opsins and those having undergone molecular engineering (see above) have gone a considerable way to mitigate effects of desensitization; however, 100 Hz stimulation remains beyond the reach of many opsins, which may impede the use of certain long-term plasticity induction protocols (though see[37]). Second, the slow kinetics of opsins may broaden action potentials[18] leading to prolonged transmitter release and vesicular depletion; this may also result from the calcium permeability of excitatory opsins[11]; these issues can be mitigated by avoiding over-bouton photoactivation[38]. Third, transduction of neurons using AAV vectors may also lead to altered presynaptic release properties in certain synapses; however, this may be mitigated by using the AAV9 serotype[38]. Despite these limitations, with careful use, optogenetic activation can mimic electrical stimulation[19,38] and is, therefore, an invaluable tool in investigating the physiology of unstudied synaptic pathways. We also note that the data shown in **Figure 3E** assess short-term plasticity in current-clamp and is, therefore, subject to interaction of synaptic potentials and intrinsic membrane properties, this can be avoided by performing equivalent experiments in voltage-clamp.

Future directions

The ever-expanding optogenetic toolbox has raised the possibility of applying this technology in two synaptic pathways in the same preparation, by using a pair of opsins with divergent excitation spectra. This is made possible by the use of an opsin ChrimsonR[26], which, unlike ChR2, is photoactivated by red wavelength light. ChrimsonR retains low-sensitivity to blue light, thus to avoid cross pathway activation it can be used in combination with red-insensitive opsins, which are violet shifted (CheRiff [27]) and/or have orders of magnitude higher sensitivity to blue light (Chronos[26]). This allows for the use of blue/violet light stimuli which are too weak to significantly activate ChrimsonR and therefore allow activation of two pathways[39,40], which may increase experimental throughput, allow examination of convergent pathway interactions, and allow the release of neuromodulators from endogenous sources[41].

ACKNOWLEDGEMENTS:

This work is supported by Wellcome grant 206401/Z/17/Z. We would like to thank Zafar Bashir for his expert mentorship and Dr. Clair Booth for technical assistance and comments on the manuscript.

DISCLOSURES:

The authors have nothing to disclose.

REFERENCES:

1. Martin, S., Grimwood, P., Morris, R. Synaptic plasticity and memory: an evaluation of the hypothesis. *Annual Review of Neuroscience*. **23**, 649–711 (2000).
2. Poorthuis, R. B. et al. Layer-specific modulation of the prefrontal cortex by nicotinic acetylcholine receptors. *Cerebral Cortex*. **23** (1), 148–161 (2013).
3. Scala, F. et al. Layer 4 of mouse neocortex differs in cell types and circuit organization between sensory areas. *Nature Communications*. **10** (1), 4174 (2019).
4. Nassar, M. et al. Diversity and overlap of parvalbumin and somatostatin expressing interneurons in mouse presubiculum. *Frontiers in Neural Circuits*. **9**, 20 (2015).
5. Dembrow, N. C., Chitwood, R. A., Johnston, D. Projection-specific neuromodulation of medial prefrontal cortex neurons. *Journal of Neuroscience*. **30** (50), 16922–16937 (2010).
6. Whitaker, L. R. et al. Bidirectional modulation of intrinsic excitability in rat prelimbic cortex neuronal ensembles and non-ensembles after operant learning. *Journal of Neuroscience*. **37** (36), 8845–8856 (2017).
7. Skrede, K. K., Westgaard, R. H. The transverse hippocampal slice: a well-defined cortical structure maintained in vitro. *Brain Research*. **35** (2), 589–593 (1971).
8. van Strien, N. M., Cappaert, N. L., Witter, M. P. The anatomy of memory: an interactive overview of the parahippocampal-hippocampal network. *Nature Reviews Neuroscience*. **10** (4), 272–282 (2009).
9. Cruikshank, S. J. et al. Thalamic control of layer 1 circuits in prefrontal cortex. *Journal of Neuroscience*. **32** (49), 17813–17823 (2012).
10. Boyden, E. S., Zhang, F., Bamberg, E., Nagel, G., Deisseroth, K. Millisecond-timescale, genetically targeted optical control of neural activity. *Nature Neuroscience*. **8** (9), 1263–1268 (2005).

11. Nagel, G. et al. Channelrhodopsin-2, a directly light-gated cation-selective membrane channel. *Proceedings of the National Academy of Sciences of the United States of America*. **100** (24), 13940–13945 (2003).
12. Berndt, A. et al. High-efficiency channelrhodopsins for fast neuronal stimulation at low light levels. *Proceedings of the National Academy of Sciences of the United States of America*. **108** (18), 7595–7600 (2011).
13. Cetin, A., Komai, S., Eliava, M., Seeburg, P. H., Osten, P. Stereotaxic gene delivery in the rodent brain. *Nature Protocols*. **1** (6), 3166–3173 (2006).
14. Segev, A., Garcia-Oscos, F., Kourrich, S. Whole-cell patch-clamp recordings in brain slices. *Journal of Visualized Experiments: JoVE*. (112) (2016).
15. Booker, S. A. Preparing acute brain slices from the dorsal pole of the hippocampus from adult rodents. *Journal of Visualized Experiments: JoVE*. (163) (2020).
16. Anderson, W. W., Collingridge, G. L. Capabilities of the WinLTP data acquisition program extending beyond basic LTP experimental functions. *Journal of Neuroscience Methods*. **162** (1–2), 346–356 (2007).
17. Basu, J. et al. Gating of hippocampal activity, plasticity, and memory by entorhinal cortex long-range inhibition. *Science*. **351** (6269), aaa5694 (2016).
18. Zhang, Y. P., Oertner, T. G. Optical induction of synaptic plasticity using a light-sensitive channel. *Nature Methods*. **4** (2), 139–141 (2007).
19. Banks, P. J., Warburton, E. C., Bashir, Z. I. Plasticity in prefrontal cortex induced by coordinated synaptic transmission arising from reuniens/rhomboid nuclei and hippocampus. *Cerebral Cortex Communications.* **2** (2), tgab029 (2021).
20. Petreanu, L., Mao, T., Sternson, S. M., Svoboda, K. The subcellular organization of neocortical excitatory connections. *Nature*. **457** (7233), 1142–1145 (2009).
21. Swietek, B., Gupta, A., Proddutur, A., Santhakumar, V. Immunostaining of biocytin-filled and processed sections for neurochemical markers. *Journal of Visualized Experiments: JoVE*. (118) (2016).
22. Jones, B. F., Witter, M. P. Cingulate cortex projections to the parahippocampal region and hippocampal formation in the rat. *Hippocampus*. **17** (10), 957–976 (2007).
23. Anastasiades, P. G., Collins, D. P., Carter, A. G. Mediodorsal and ventromedial thalamus engage distinct L1 circuits in the prefrontal cortex. *Neuron*. **109** (2), 314–330 e314 (2021).
24. Prakash, R. et al. Two-photon optogenetic toolbox for fast inhibition, excitation and bistable modulation. *Nature Methods*. **9** (12), 1171–1179 (2012).
25. Mattis, J. et al. Principles for applying optogenetic tools derived from direct comparative analysis of microbial opsins. *Nature Methods*. **9** (2), 159–172 (2011).
26. Klapoetke, N. C. et al. Independent optical excitation of distinct neural populations. *Nature Methods*. **11** (3), 338–346 (2014).
27. Hochbaum, D. R. et al. All-optical electrophysiology in mammalian neurons using engineered microbial rhodopsins. *Nature Methods*. **11** (8), 825–833 (2014).
28. Ting, J. T., Daigle, T. L., Chen, Q., Feng, G. Acute brain slice methods for adult and aging animals: application of targeted patch clamp analysis and optogenetics. *Methods in Molecular Biology*. **1183**, 221–242 (2014).
29. Marshel, J. H. et al. Cortical layer-specific critical dynamics triggering perception. *Science*. **365** (6453) (2019).

30. Castle, M. J., Gershenson, Z. T., Giles, A. R., Holzbaur, E. L., Wolfe, J. H. Adeno-associated virus serotypes 1, 8, and 9 share conserved mechanisms for anterograde and retrograde axonal transport. *Human Gene Therapy*. **25** (8), 705–720 (2014).
31. Aschauer, D. F., Kreuz, S., Rumpel, S. Analysis of transduction efficiency, tropism and axonal transport of AAV serotypes 1, 2, 5, 6, 8 and 9 in the mouse brain. *PLoS One*. **8** (9), e76310 (2013).
32. Nathanson, J. L., Yanagawa, Y., Obata, K., Callaway, E. M. Preferential labeling of inhibitory and excitatory cortical neurons by endogenous tropism of adeno-associated virus and lentivirus vectors. *Neuroscience*. **161** (2), 441–450 (2009).
33. Dimidschstein, J. et al. A viral strategy for targeting and manipulating interneurons across vertebrate species. *Nature Neuroscience*. **19** (12), 1743–1749 (2016).
34. Lavin, T. K., Jin, L., Lea, N. E., Wickersham, I. R. Monosynaptic tracing success depends critically on helper virus concentrations. *Frontiers in Synaptic Neuroscience*. **12**, 6 (2020).
35. Paxinos, G., Watson, C. *The Rat Brain in Stereotaxic Coordinates*. 7th edn, Academic Press (2013).
36. Paxinos, G., Franklin, K. B. J. *Paxinos and Franklin's the Mouse Brain in Stereotaxic Coordinates, Compact*. 5th edn, Academic Press (2019).
37. Nabavi, S. et al. Engineering a memory with LTD and LTP. *Nature*. **511** (7509), 348–352 (2014).
38. Jackman, S. L., Beneduce, B. M., Drew, I. R., Regehr, W. G. Achieving high-frequency optical control of synaptic transmission. *Journal of Neuroscience*. **34** (22), 7704–7714 (2014).
39. Xia, S. H. et al. Cortical and Thalamic Interaction with Amygdala-to-Accumbens Synapses. *Journal of Neuroscience*. **40** (37), 7119–7132 (2020).
40. Anisimova, M. et al. Spike-timing-dependent plasticity rewards synchrony rather than causality. *BioRxiv* (2021).
41. Takeuchi, T. et al. Locus coeruleus and dopaminergic consolidation of everyday memory. *Nature*. **537** (7620), 357–362 (2016).

FIGURE LEGENDS:

Figure 1: Experimental overview. (**A**) Schematic of viral vector injection into medial prefrontal cortex (mPFC), transduction of mPFC cells with optogenetic construct, and transport of construct to terminals in lateral entorhinal cortex (LEC). (**B**) Schematic representation of whole-cell recording from layer 5 pyramidal neurons in an acute LEC slice and light activation of mPFC terminals *via* microscope objective. Abbreviations: CA = cornu ammonis; PERI = perirhinal cortex; TR = transition region.

Figure 2: Slice collection chamber and optical configuration for visualized whole-cell recordings, optogenetic excitation, and identification of tdTomato positive neurons. (**A**) The slice collection chamber[14] is custom made from a microcentrifuge tube rack glued onto a sheet of nylon mesh and placed into a beaker in which it is submerged in aCSF (**B**) LEDs for excitation of ChR2 (470 nm) and tdTomato (565 nm) are directed through an aspherical condenser lens to collimate light, 565 nm light is beamed through a band-pass filter to achieve spectral separation of tdTomato excitation and emission spectra. These are combined with a long-pass dichroic mirror and directed toward the slice with a second long-pass dichroic mirror of a longer wavelength. Light is then focused on the slice *via* the objective lens. In experiments where tdTomato labeled neurons are present, emitted fluorescent light passes through the dichroic mirror and emission filter and is focused onto the camera sensor by an achromatic lens. Non-fluorescent features of the slice are visualized by oblique refracted near infra-red (NIR) light applied from under the slice chamber; this light passes the optics to the camera thus negating the need to change filter-cubes between fluorescent and NIR imaging.

Figure 3: Visualization of neurons under NIR/fluorescent imaging and representative examples of oEPSPs. (**A**) Left: Example of neuron with pyramidal morphology visualized with NIR light. Right: Same neuron with the formation of concave dimple caused by positive pressure from the patch pipette. (**B**) Cre-recombinase dependent expression of tdTomato in a single neuron. (**C**) Representative oEPSP from LEC layer 5 in the pyramidal cell. (**D**) Example of long-term plasticity experiment monitoring oEPSP over time following addition of 10 µm carbachol (CCh). The dotted line indicates average oEPSP amplitude during baseline period before drug addition. (**E**) Representative traces of trains of stimulation at 5, 10, and 20 Hz. Blue arrows denote light activation. Scale bars = 20 µm.

Figure 4: Histological verification of injection site and recovery of biocytin filled cell. (**A**) Coronal photomicrograph showing viral injection site in mPFC, +3.00 mm from bregma. (**B**) Thin coronal section of LEC illustrating mCherry+ fibers. (**C**) Low power image of 350 µm thick acute slice, -6.2 mm from bregma, with biocytin filled pyramidal cell in LEC. The dashed box is shown at higher magnification in D. (**D**) LEC pyramidal cell; the apical dendrite can be seen on the right of the image heading toward layer 1. Dashed lines denote regional borders. Abbreviations: IL = infralimbic cortex; PL = prelimbic cortex; wm = white matter. Scale bars = 250 µm.

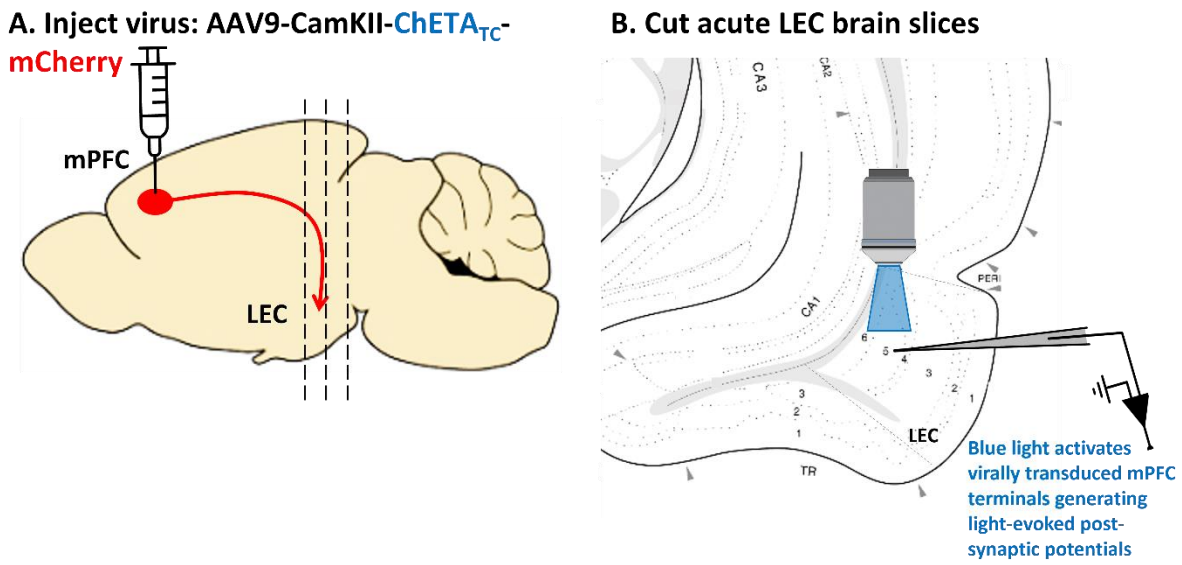
A. Inject virus: AAV9-CamKII-ChETA$_{TC}$-mCherry
mPFC
LEC
B. Cut acute LEC brain slices
CA3
CA2
CA1
PER
LEC
TR
Blue light activates virally transduced mPFC terminals generating light-evoked post-synaptic potentials

Figure 1.

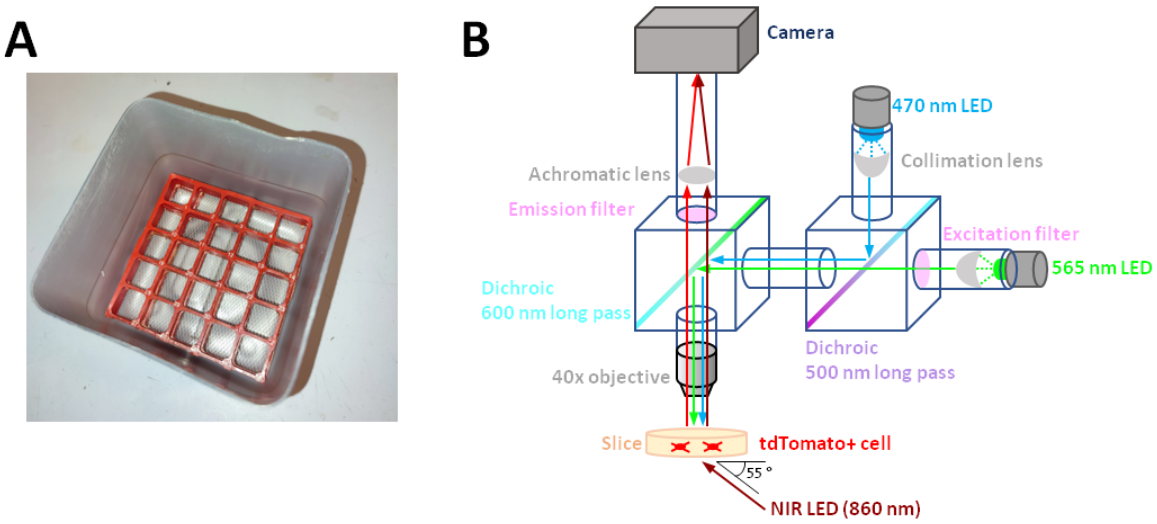
A
B
Camera
470 nm LED
Collimation lens
Achromatic lens
Emission filter
Excitation filter
565 nm LED
Dichroic
600 nm long pass
Dichroic
500 nm long pass
40x objective
Slice
tdTomato+ cell
55 °
NIR LED (860 nm)

Figure 2.

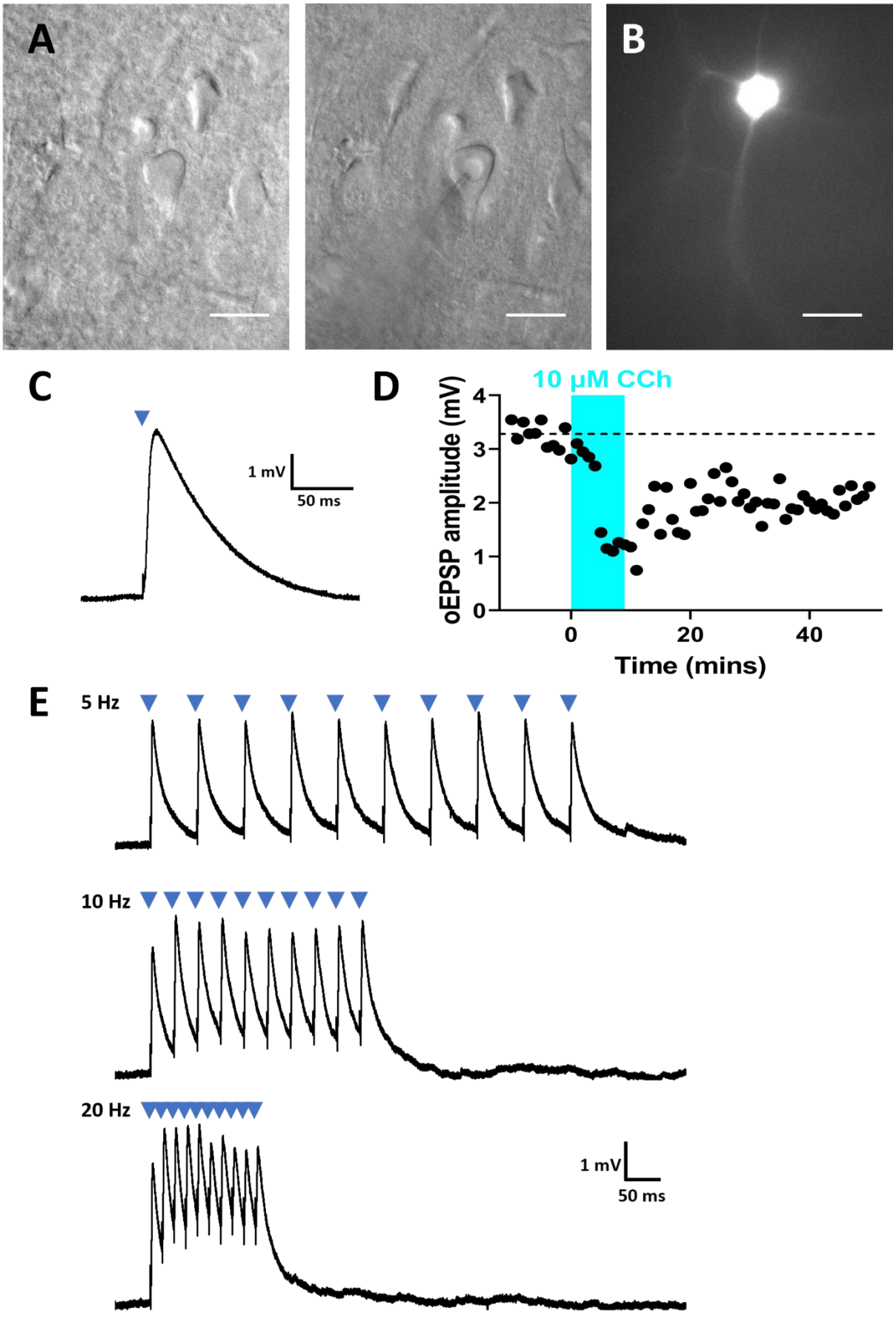
A
B
C
1 mV
50 ms
D
10 µM CCh
oEPSP amplitude (mV)
0
1
2
3
4
0
20
40
Time (mins)
E
5 Hz
10 Hz
20 Hz
1 mV
50 ms

Figure 3.

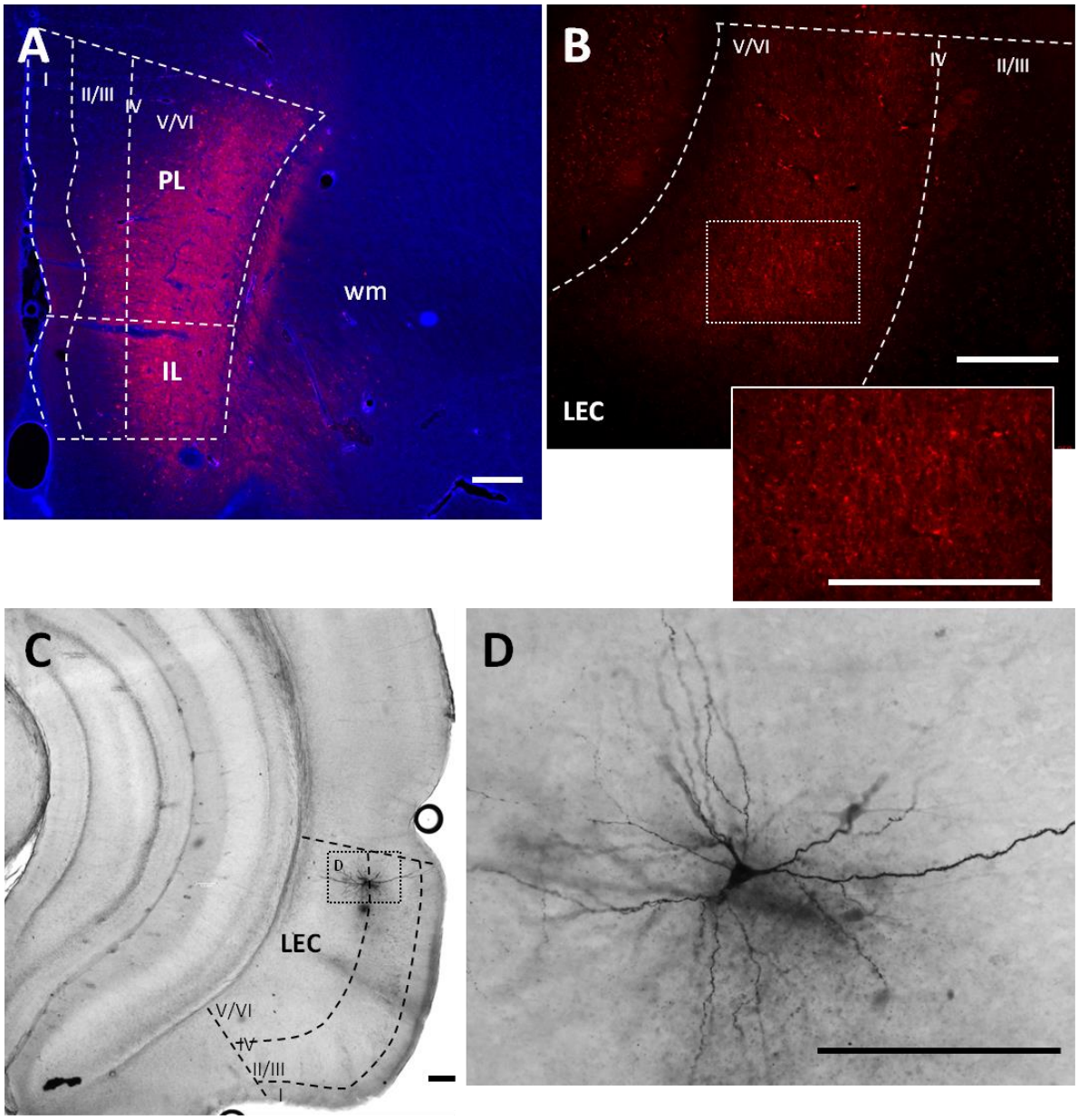

Figure 4.